

Supporting Information

The synthesis of DHAD/ZnAlTi-LDH composite with advanced UV blocking and antibacterial activity for skin protection

Xinlong Liu,^a Tingting Hu,^b Guishan Lin,^a Xiu Wang,^a Yu Zhu,^b Ruizheng Liang,^{*b} Wengui Duan,^{*a} and Min Wei^b

^a School of Chemistry and Chemical Engineering, Guangxi University, Nanning 530004, Guangxi, China

^b State Key Laboratory of Chemical Resource Engineering, Beijing Advanced Innovation Center for Soft Matter Science and Engineering, Beijing University of Chemical Technology, Beijing 100029, P. R. China

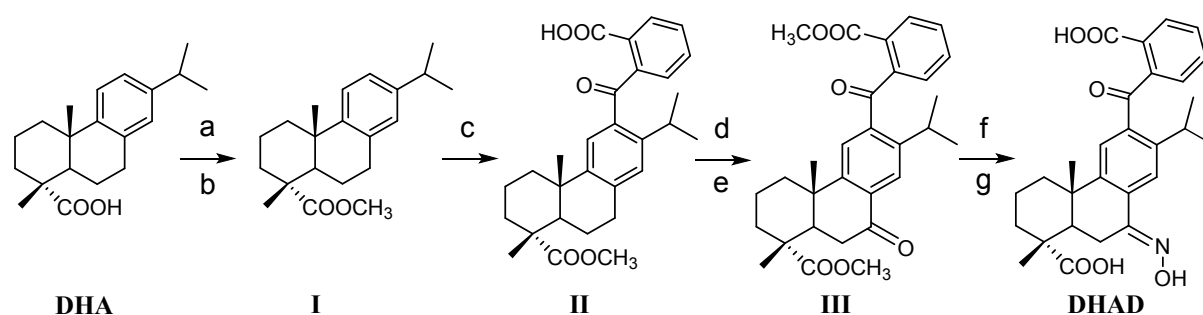
E-mail: wgduan@gxu.edu.cn (W. Duan); liangrz@mail.buct.edu.cn (R. Liang)

Experimental Section

1. Synthesis of LDH.

LDH nanosheets were prepared by a bottom-up method. Briefly, solution A: $\text{Zn}(\text{NO}_3)_2 \cdot 6\text{H}_2\text{O}$ (0.4 mmol), $\text{Al}(\text{NO}_3)_3 \cdot 9\text{H}_2\text{O}$ (0.02, 0.04, 0.06 mmol, respectively) and TiCl_4 (0.18, 0.16, 0.14 mmol, respectively) dissolved in deionized water (40 mL). Solution B: NaNO_3 (0.2 mmol) dissolved in 40 mL of deionized water containing 25% formamide. Solution C: NaOH (4.5 mmol) dissolved in deionized water (30 mL). Solution A and solution C were added slowly into solution B with stirring at 80 °C for 30 min, and the resulting LDH nanosheets were centrifuged, followed by further dialysis (3 kDa) to remove formamide.

2. Synthesis of DHAD.



Scheme S1. Synthetic pathway to targeted compounds. Reagents and conditions: (a) Benzene, SOCl_2 , 80 °C, 3 h. (b) CH_3OH , 80 °C, 3 h. (c) *o*-Phthalic anhydride, DCM, AlCl_3 , rt, 6 h. (d) Benzene, SOCl_2 , 80 °C, 3 h. then, CH_3OH , 80 °C, 3 h. (e) CrO_3 , CH_3COOH , 80 °C, 9 h. (f) hydroxylamine hydrochloride, $\text{CH}_3\text{CH}_2\text{OH}$, Et_3N , 80 °C, 8 h. (g) KOBu^t , DMSO, 70 °C, 5 h.

Compound I was synthesized according to the literature.^{1,2} And compound II was synthesized by the following method. Under an ice salt bath, 3 mmol of anhydrous AlCl_3 and 1.5 mmol of *o*-Phthalic anhydride were added to 30 mL of dry DCM, and the mixture was stirred for 30 min, then, 1 mmol of compound I was added into the mixture. The reaction mixture was stirred at room temperature for 6 h. After the reaction is over, the reaction mixture was poured into ice water and added 10 mL HCl (1 N) into the ice water. Then the reaction mixture extracted with DCM. The organic layer was washed with H_2O and brine, dried over anhydrous Na_2SO_4 , filtered, and then the solvent was evaporated in a vacuum. The crude mixture was purified by flash chromatography (petroleum ether/ethyl acetate = 6: 1, v/v) to afford compound II as a colorless solid. Yield 56%.

Reaction e:

After methyl esterification protection of compound II, the intermediate was added dropwise to a solution of CrO_3 (3 mmol) in Ac_2O (9 mL) and AcOH (4 mL) at room temperature. The reaction mixture was stirred at 80 °C for 9 h. After the reaction is over, the mixture was

extracted with CHCl_3 3 times. The combined organic layer was washed with water, NaHCO_3 , and brine, and dried over Na_2SO_4 . The crude mixture was purified by silica gel column chromatography (petroleum ether/ethyl acetate = 3: 1, v/v) to afford compound III as a yellow solid. Yield 71%.

Reaction f:

Compounds III (1 mmol) and hydroxylamine hydrochloride (1.5 mmol) were added to ethanol (15 mL) and the mixture was stirred at 80 °C for 8 h. After the reaction was completed, the solvent was evaporated under reduced pressure, and the crude product was purified by chromatography on silica gel eluting with petroleum ether/ethyl acetate (4: 1, v/v) to obtain the intermediate.

Reaction g:

The intermediate (1 mmol) come from **Reaction f** was treated with KOBU^t (3 mmol) in DMSO (20 mL) at 80 °C for about 5 h. Then the reaction mixture was poured into ice water, acidified with 1 N HCl, and then extracted with AcOEt. The combined organic layer was washed with H_2O and brine, dried over anhydrous Na_2SO_4 , filtered, and then the solvent was evaporated in a vacuum. The crude residue was purified by column chromatography using petroleum ether/ethyl acetate (2: 1, v/v). Yield 67%.

3. Synthesis of DHAD/ZnAlTi-LDH composite.

DHAD was firstly dissolved in EtOH, LDH nanosheets colloid was mixed with DHAD solution with various mass ratios (from LDH: DHAD = 4: 1 to LDH: DHAD = 1: 4), and stirred for 6 h at room temperature. The resulting DHAD/ZnAlTi-LDH was obtained by centrifugation at 9000 rpm for 6 min. The product was dried in vacuum at 60 °C for 6 h after being washed by the distilled water 3 times.

4. Antibacterial activity *in vitro*.

Wide-type *E. coli* (ATCC 25922) and *S. aureus* (ATCC 22004) were used as the models of Gram-negative and Gram-positive bacterium strains, respectively.³ The bacteria were grown on the standard beef-peptone-yeast (BPY) agar plate at 37°C, cultured to the log phase with shaking for 6 h, harvested by a centrifugation at 8000 rpm, washed with phosphate buffer saline (PBS, 10 mM, pH = 7.4), and then suspended in PBS to a concentration of $\sim 5 \times 10^4$ CFU mL^{-1} . Then bacteria were incubated separately with DHAD, ZnAlTi-LDH, DHAD/ZnAlTi-LDH (final concentration: 0.2 mg mL^{-1}) in PBS for 6 h, and then exposed to a solar simulator for different time (0, 5, 10, 20 and 40 min, 100 mW cm^{-2} , 400-780 nm). The bacteria sample only treated with light exposure was set as a control group. The bacterial concentration was measured at different times of light exposure using standard spread-plating techniques. Each group was gradiently diluted and each dilution in triplicate was plated onto

the trypticase soy agar culture medium and incubated for 18 h. Bacteria survival rate was calculated using the following equation:

$$\% \text{ survival} = C/C_0 \times 100\%$$

where C is the terminal concentration of bacteria and C_0 is the concentration at $t = 0$ of the experiments.

5. *In vivo* antibacterial activity and wound healing.

Balb/c mice (female, 6 weeks, 18-21 g body weight) were obtained from Vital River Corp. All animal studies were conducted under the guidelines of the National Institute of Health Guiding Principles for the Care and Use of Laboratory Animals, and the overall project protocols were approved by the Ethics Review Committee for Animal Experimentation of the Institute of Clinical Medicine, China-Japan Friendship Hospital, Beijing. The dorsal hair of mice was shaved and their dorsal skin was cleaned with 70% alcohol. A rounded full-thickness skin wound was created by excising the dorsum of the animals on the backside. The wounds were infected with 10 μL (10^6 CFU mL^{-1}) *S. aureus* and bandaged with elastic bandages. Four hours later, the wound was treated with different methods. The *S. aureus* infected wound was treated with (i) PBS (control), (ii) PBS + light (100 mW cm^{-2}), (iii) DHAD/ZnAlTi-LDH, (iv) DHAD/ZnAlTi-LDH + light (100 mW cm^{-2}), (v) Commercial anti-inflammatory drugs (Mupirocin). Then, the animals were individually housed in cages and allowed to heal. The wound size of the animals was recorded daily. In order to increase the adhesion, carboxy methyl cellulose (CMC) was chosen as a thickener. LDH and a certain amount of CMC can be uniformly mixed under ultrasonic.

6. Anti-UV evaluation *in vivo*.

Balb/c mice (female, 6 weeks, 18-21 g body weight) were obtained from Vital River Corp. The dorsal skin was cleaned with 70% alcohol. The group without UV exposure was used as the control group and other groups were treated with PBS, sunscreen (Dabao sunscreen lotion, SPF 30), DHAD/ZnAlTi-LDH ($200 \mu\text{g mL}^{-1}$, mixed with CMC), and exposed to the UV lamp (280-320 nm, 0.1 mW cm^{-2}) for 2 hours per day. Ten days after UV exposure, the dorsal skin was removed and prepared for histology.

7. Sample characterization.

Powder X-ray diffraction patterns of the samples were collected on a Shimadzu XRD-6000 diffractometer using a Cu $K\alpha$ source, with a scan step of 0.02° and a scan range between 3° - 70° . The particle size distribution and zeta potential were determined using a Malvern Mastersizer 2000 laser particle size analyzer. The Fourier transform infrared (FT-IR) spectra were recorded using a Vector 22 (Bruker) spectrophotometer using the KBr pellet technique in the range 4000 - 400 cm^{-1} with 1 cm^{-1} resolution. The UV-vis absorption spectra were

collected in the range 200-800 nm on a Shimadzu U-3000 spectrophotometer, with a slit width of 1.0 nm. Fluorescence images of these samples were obtained using an Olympus 1X71 fluorescence microscope with 400 folds enlargement. The XPS spectrum of LDH nanosheets was investigated via a PHI Q2000 X-ray photoelectron spectrometer with an Al K X-ray source. The morphology of LDH was studied on a high-resolution transmission electron microscope (HRTEM, JEOL, JEM-2100, 200 kV). The thickness of LDH and DHAD/LDH was recorded on an atomic force microscope (AFM, Veeco, NanoScope IIIa) with the tapping mode. The GC analysis was conducted on an Agilent 6890 GC (Agilent Technologies Inc., Santa Clara, CA, USA) equipped with an HP-1 column (30 m, 0.530 mm, 0.88 μ m) and FID. NMR spectra were recorded in CDCl₃ solutions on a Bruker Avance III HD 600 MHz spectrometer (Bruker Co., Ltd., Zurich, Switzerland) and chemical shifts are expressed in ppm (δ) downfield relative to TMS as an internal standard. MS spectra were obtained by means of the electrospray ionization (ESI) method on the TSQ Quantum Access MAX HPLC-MS instrument (Thermo Scientific Co., Ltd., Waltham, MA, USA).

Supplementary Figures

Compound II (2-((4bS, 8R)-2-isopropyl-8-(methoxycarbonyl)-4b,8-dimethyl-4b,5,6,7,8,8a,9,10-octahydrophenanthrene-3-carbonyl) benzoic acid):

^1H NMR (600 MHz, CDCl_3) δ 8.00-7.99 (d, 1H), 7.63-7.61 (t, 1H), 7.58-7.56 (t, 1H), 7.43-7.42 (d, 1H), 7.11 (s, 1H), 7.06 (s, 1H), 3.74-3.69 (m, 1H), 3.67 (s, 3H), 2.93-2.91 (m, 2H), 2.20-2.18 (d, 1H), 1.88-1.81 (m, 2H), 1.72-1.70 (m, 2H), 1.62-1.60 (m, 2H), 1.44-1.42 (m, 2H), 1.32-1.30 (m, 1H), 1.26-1.25 (d, 6H), 1.23-1.22 (d, 3H), 1.09 (s, 3H).

^{13}C NMR (151 MHz, CDCl_3) δ 198.66, 179.03, 171.61, 147.40, 146.02, 143.62, 139.76, 134.09, 132.22, 130.54, 129.95, 129.37, 128.88, 127.69, 127.21, 51.99, 47.54, 44.66, 37.40, 36.74, 36.54, 30.09, 28.53, 24.94, 24.18, 24.01, 21.42, 18.35, 16.46. ESI-MS m/z calculated for $[\text{C}_{29}\text{H}_{34}\text{O}_5 + \text{H}]^+$ 463.2406, found 463.2484.

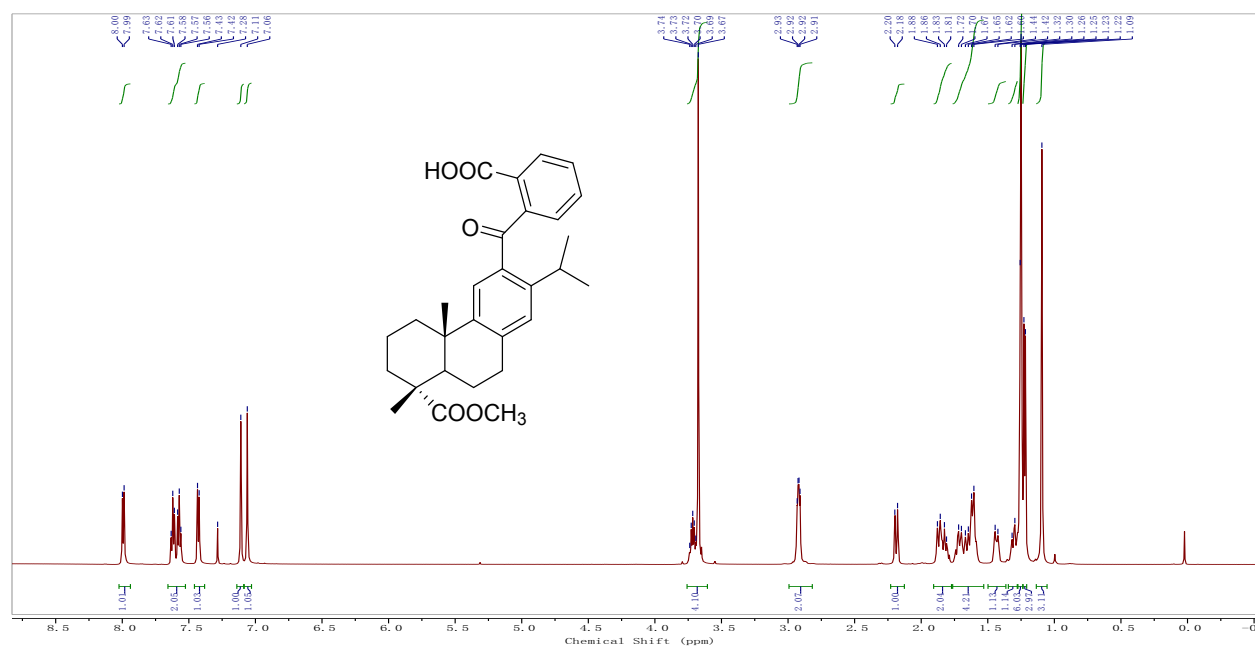


Figure S1. ^1H -NMR spectrum of compound II in CDCl_3

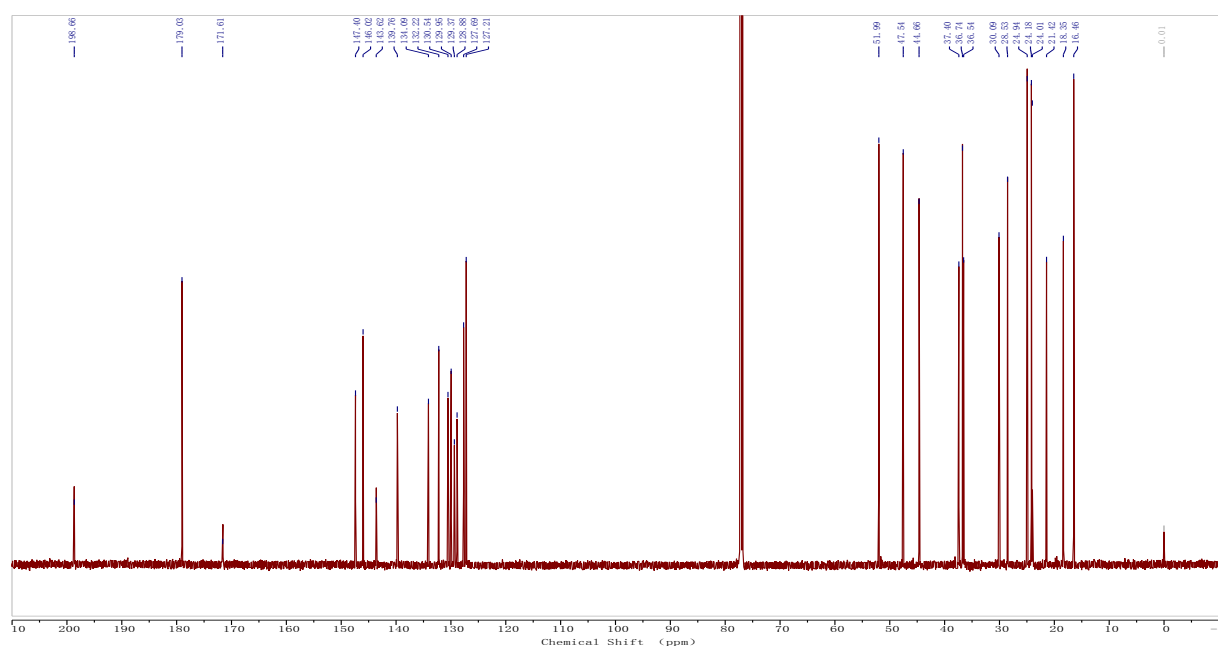


Figure S2. ^{13}C -NMR spectrum of compound II in CDCl_3

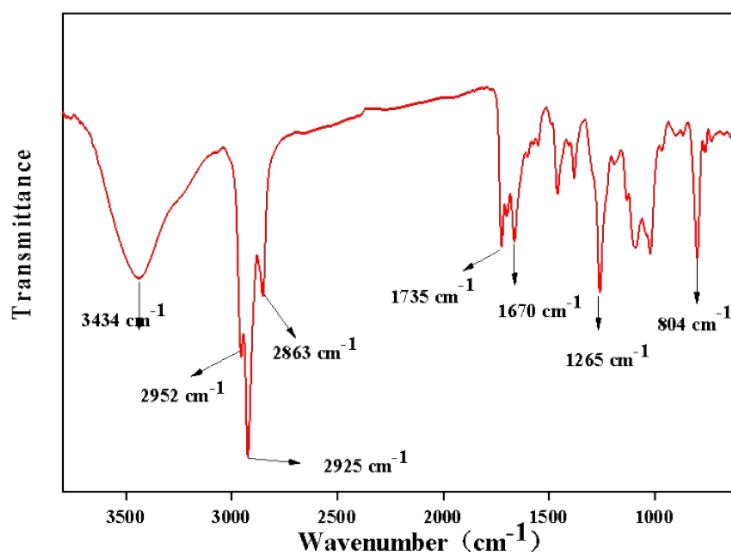


Figure S3. FT-IR spectrum of compound II

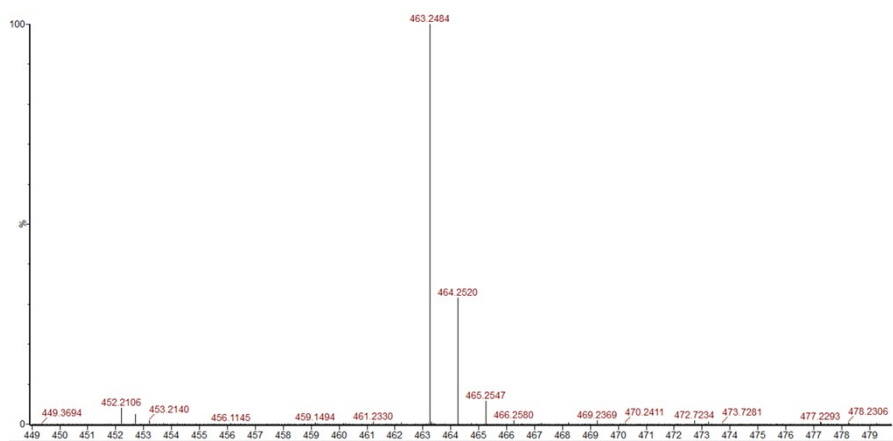


Figure S4. ESI-MS spectrum of compound II (M/Z)

Compound III (methyl (1R,4aS)-7-isopropyl-6-(2-(methoxycarbonyl)benzoyl)-1,4a-dimethyl-9-oxo-1,2,3,4,4a,9,10,10a-octahydrophenanthrene-1-carboxylate):

^1H NMR (600 MHz, CDCl_3) δ 8.03 (s, 1H), 7.76-7.75 (d, 1H), 7.55-7.52 (m, 2H), 7.51-7.50 (d, 1H), 7.14 (s, 1H), 3.64 (s, 3H), 3.59 (s, 3H), 3.41-3.38 (m, 1H), 2.68-2.64 (m, 2H), 2.34-2.31 (d, 1H), 1.99 (m, 1H), 1.68-1.63 (m, 4H), 1.41 (m, 1H), 1.26-1.12 (m, 12H).

^{13}C NMR (151 MHz, CDCl_3) δ 197.72, 197.56, 177.52, 167.74, 151.83, 147.19, 141.75, 140.35, 140.34, 132.35, 131.76, 131.28, 131.22, 129.45, 125.46, 124.90, 52.44, 52.13, 46.50, 43.60, 37.74, 37.15, 36.60, 36.40, 29.33, 23.99, 23.87, 23.44, 17.88, 16.28. ESI-MS m/z calculated for $[\text{C}_{30}\text{H}_{34}\text{O}_6 + \text{H}]^+$ 491.2355, found 491.2422.

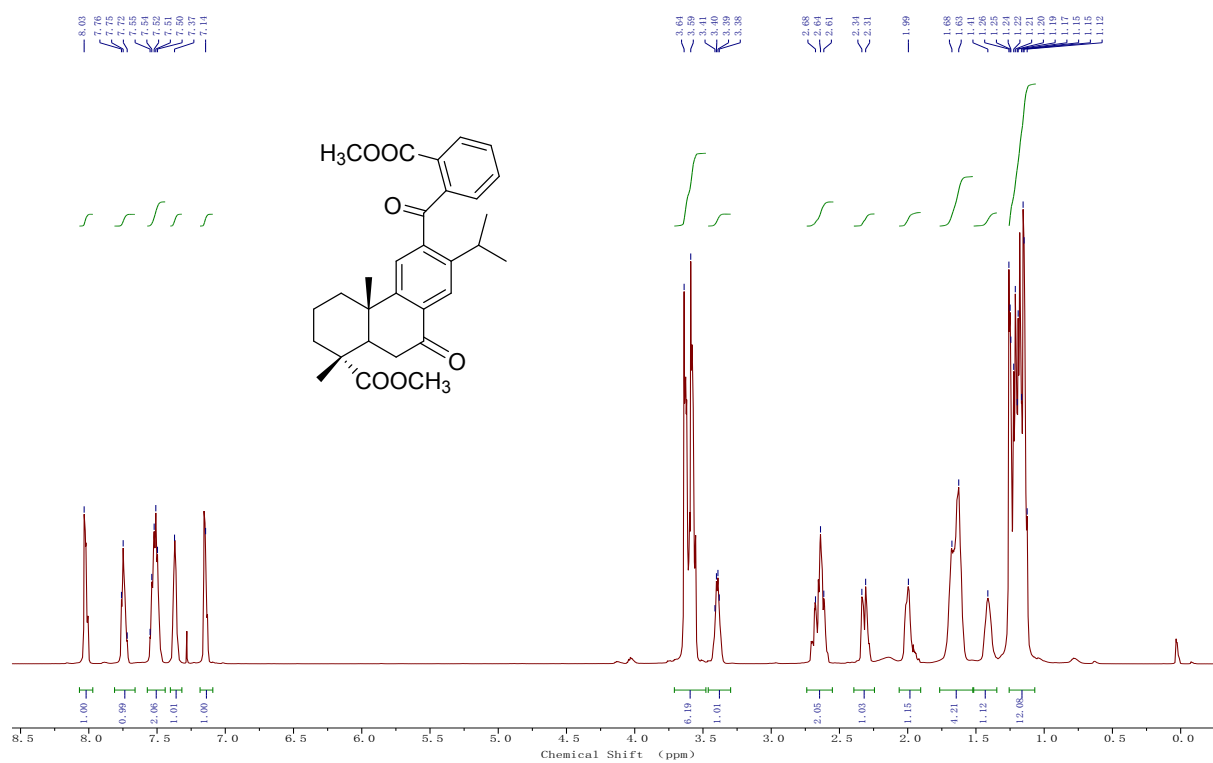


Figure S5. ¹H-NMR spectrum of compound III in CDCl₃

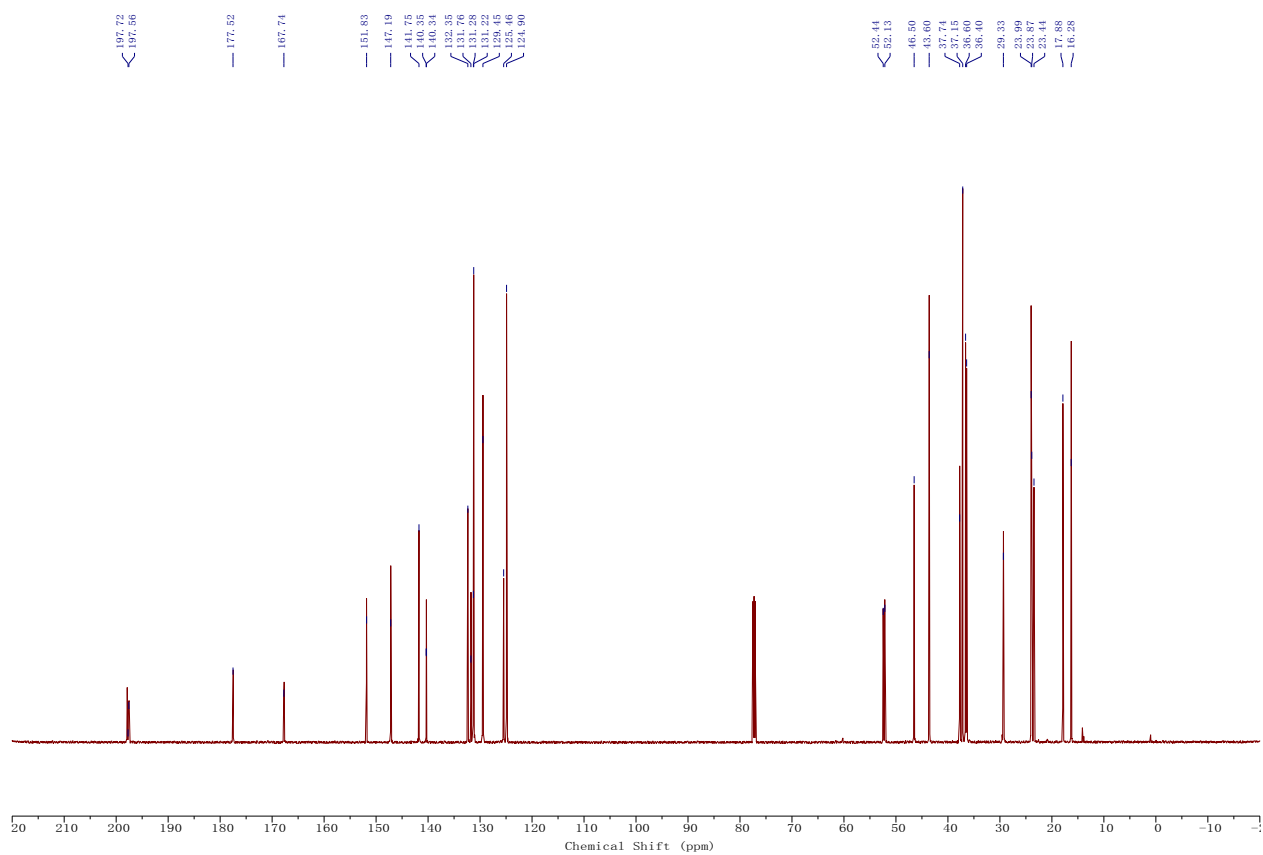


Figure S6. ¹³C-NMR spectrum of compound III in CDCl₃

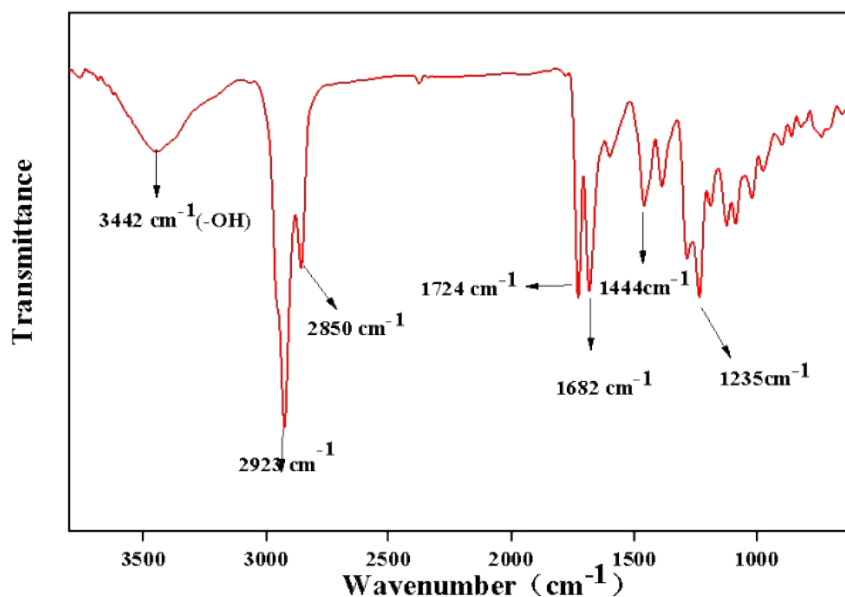


Figure S7. FT-IR spectrum of compound III

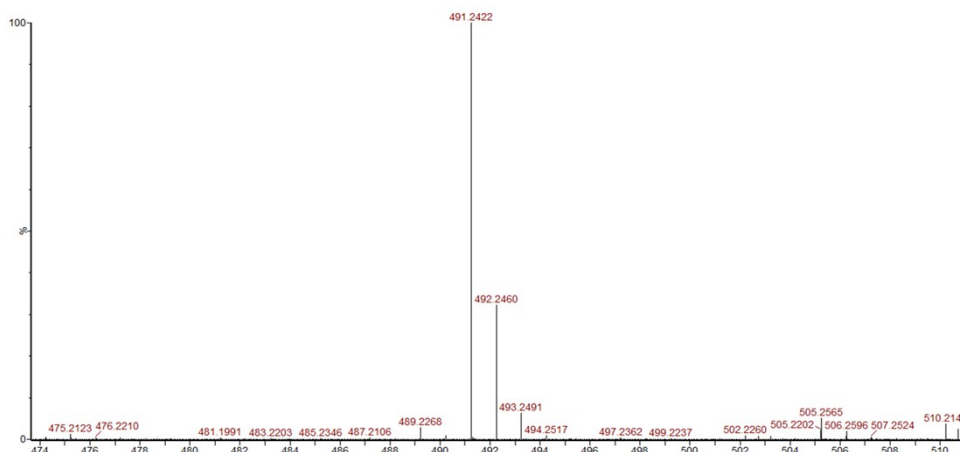


Figure S8. ESI-MS spectrum of compound III (M/Z)

DHAD ((1R,4aS,E)-6-(2-carboxybenzoyl)-9-(hydroxyimino)-7-isopropyl-1,4a-dimethyl-1,2,3,4,4a,9,10,10a-octahydrophenanthrene-1-carboxylic acid):

^1H NMR (600 MHz, CDCl_3) δ 8.13 (s, 1H), 8.01-7.99 (d, 1H), 7.70-7.68 (t, 1H), 7.64-7.59 (m, 2H), 6.89 (s, 1H), 5.97 (s, 1H), 3.59-3.54 (m, 1H), 2.78-2.72 (m, 1H), 2.24-2.16 (m, 2H), 1.78-1.76 (d, 1H), 1.70-1.64 (d, 2H), 1.59-1.48 (m, 3H), 1.42-1.41 (d, 3H), 1.35-1.34 (d, 3H), 1.25 (s, 3H), 0.99 (s, 3H).

^{13}C NMR (151 MHz, CDCl_3) δ 196.64, 185.19, 174.36, 158.28, 148.14, 146.70, 139.54, 138.38, 134.28, 131.74, 131.54, 131.35, 130.34, 127.87, 125.14, 122.78, 46.39, 40.28, 38.50, 35.92, 35.44, 29.23, 25.91, 24.93, 22.32, 22.18, 17.61, 16.23. ESI-MS m/z calculated for $[\text{C}_{28}\text{H}_{31}\text{NO}_6 + \text{H}]^+$ 478.2151, found 478.2225.

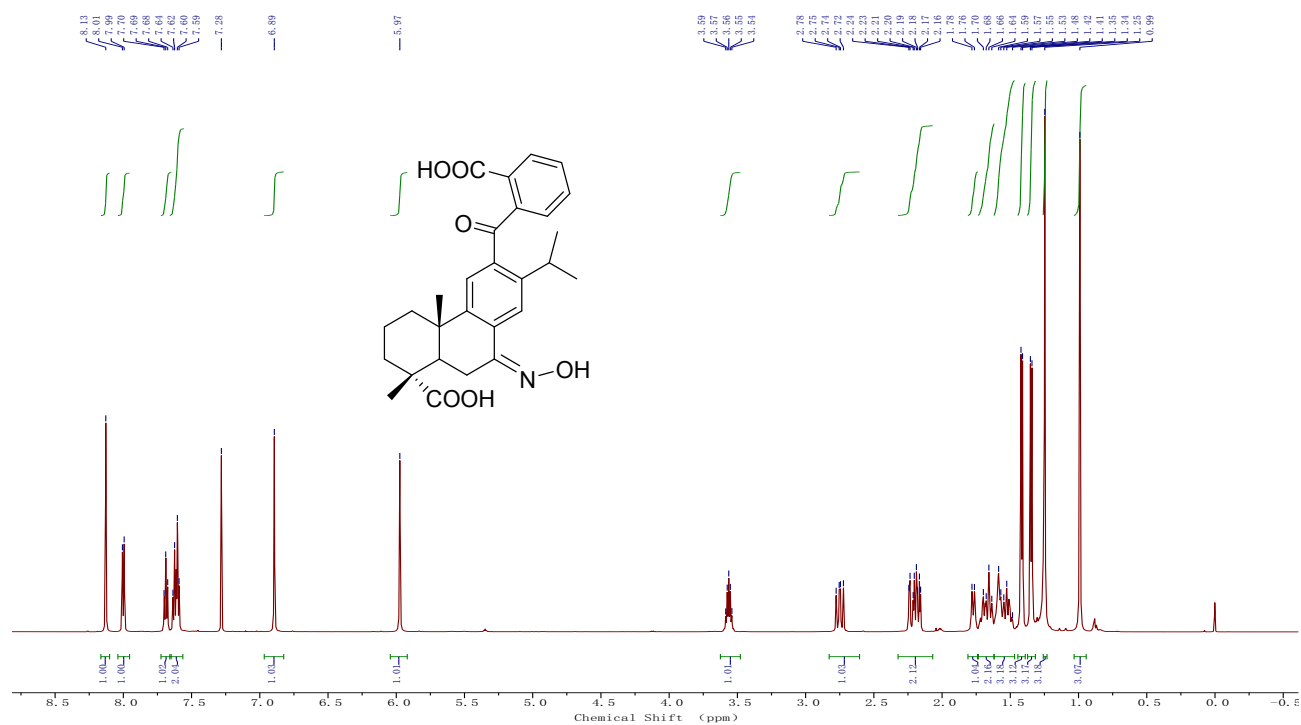


Figure S9. ^1H -NMR spectrum of DHAD in CDCl_3

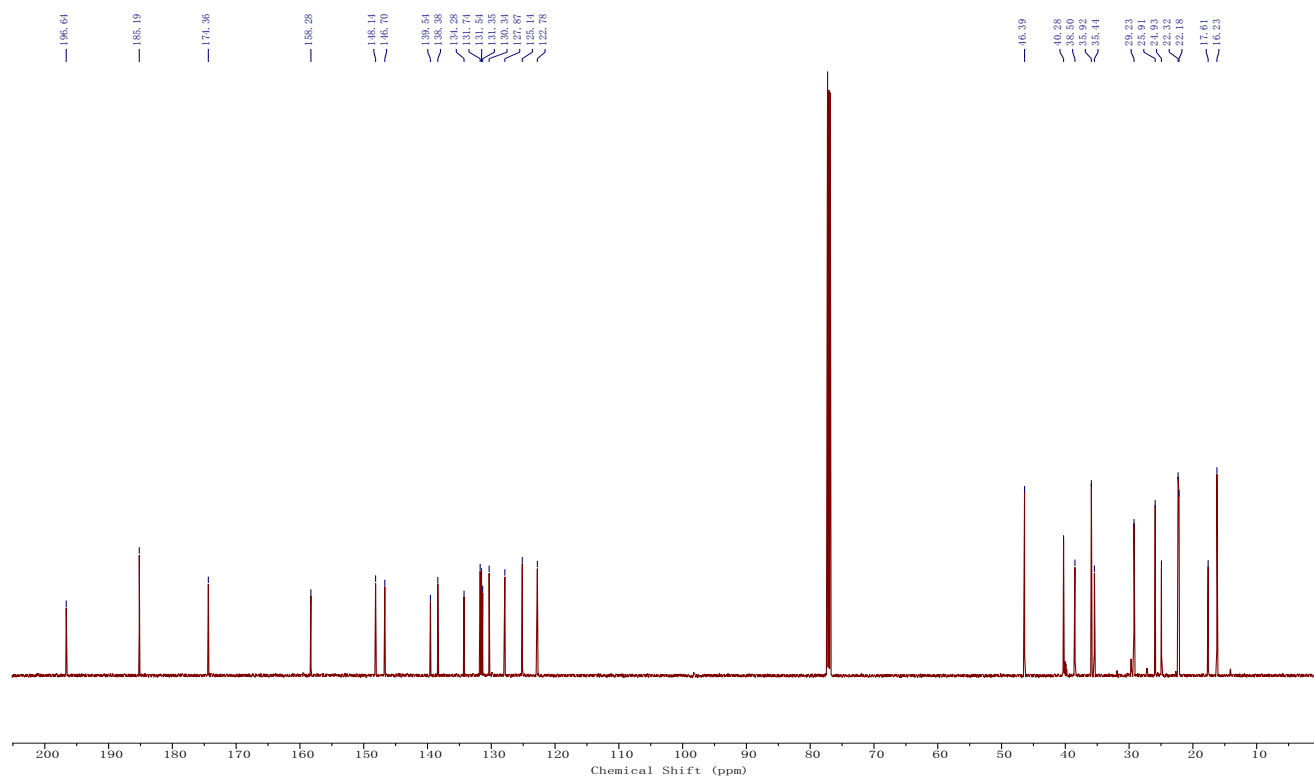


Figure S10. ^{13}C -NMR spectrum of DHAD in CDCl_3

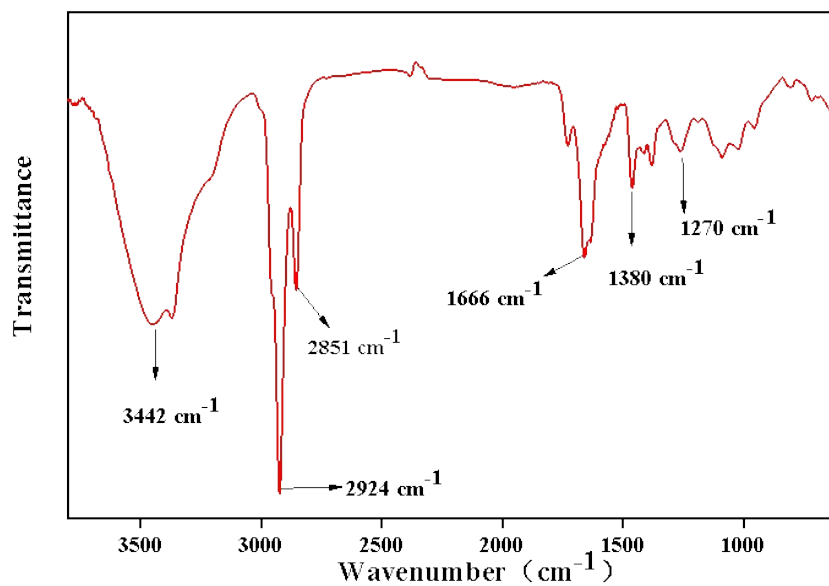


Figure S11. FT-IR spectrum of DHAD

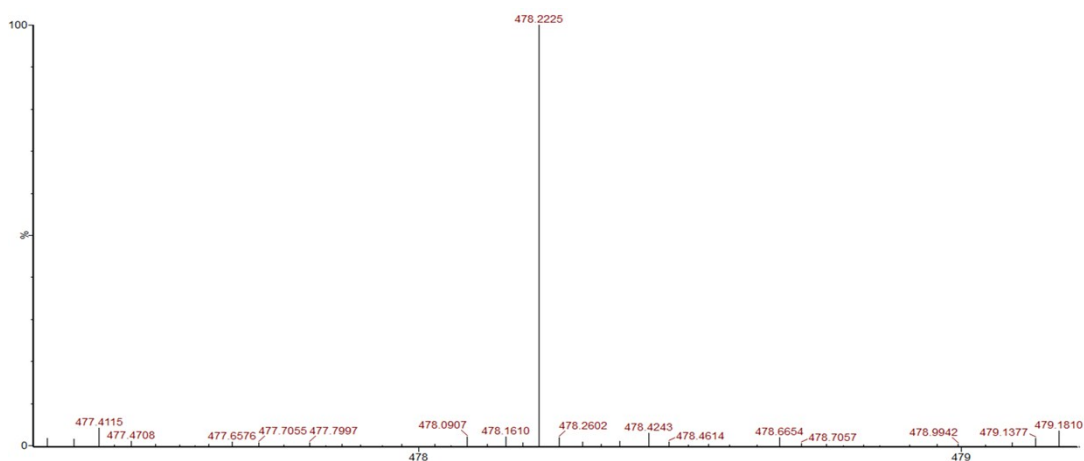


Figure S12. ESI-MS spectrum of DHAD (M/Z)

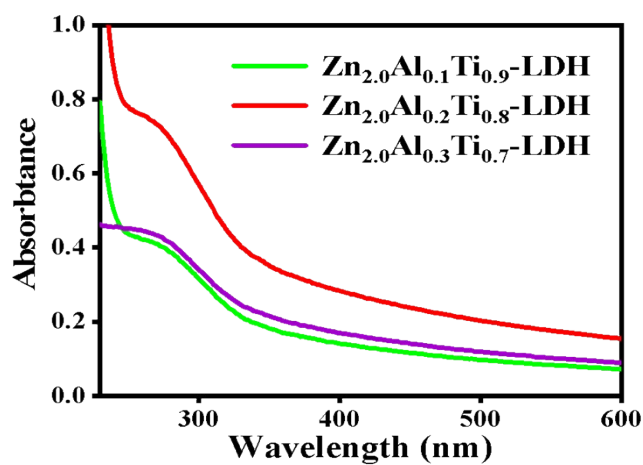


Figure S13. UV-vis absorption spectra of ZnAlTi-LDH with different ratios.

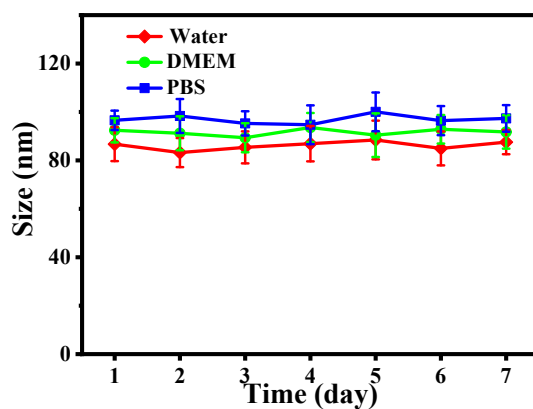


Figure S14. The particle size of ZnAlTi-LDH nanosheets in water, PBS or DMEM for 7 days.

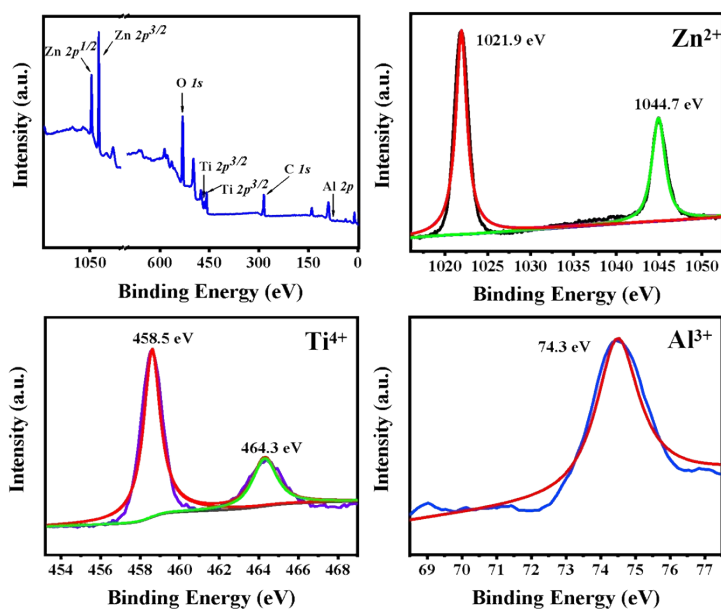


Figure S15. XPS spectra of LDH nanosheets sample. (A) Wide XPS spectra of ZnAlTi-LDH, (B) Zn^{2+} , (C) Ti^{4+} , (D) Al^{3+} .

Table S1. Chemical composition of LDH samples based on ICP results

Feed ratio	ICP results
$\text{Zn}_{2.0}\text{Ti}_{0.9}\text{Al}_{0.1}$	$\text{Zn}_{2.07}\text{Ti}_{0.89}\text{Al}_{0.11}$
$\text{Zn}_{2.0}\text{Ti}_{0.8}\text{Al}_{0.2}$	$\text{Zn}_{2.09}\text{Ti}_{0.79}\text{Al}_{0.21}$
$\text{Zn}_{2.0}\text{Ti}_{0.7}\text{Al}_{0.3}$	$\text{Zn}_{2.11}\text{Ti}_{0.70}\text{Al}_{0.35}$
$\text{Zn}_{2.0}\text{Ti}_{1.0}$	$\text{Zn}_{2.11}\text{Ti}_{1.05}$

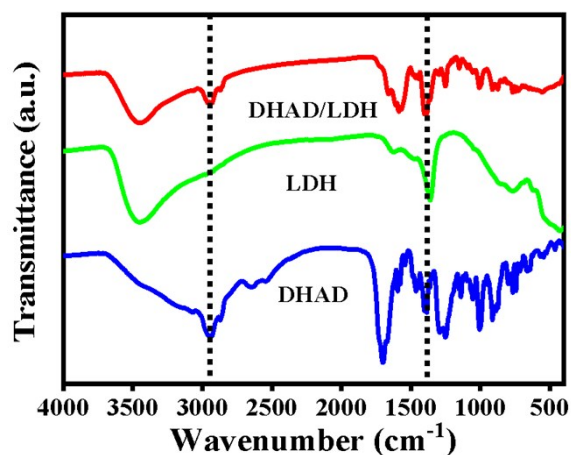


Figure S16. FT-IR spectra of DHAD, LDH, and DHAD/LDH respectively.

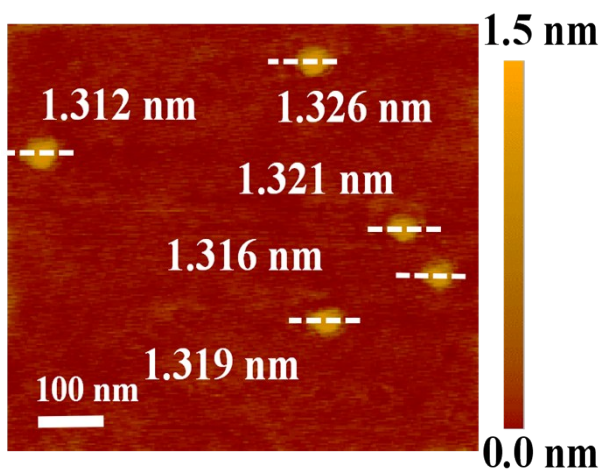


Figure S17. The thickness of DHAD/LDH nanosheets.

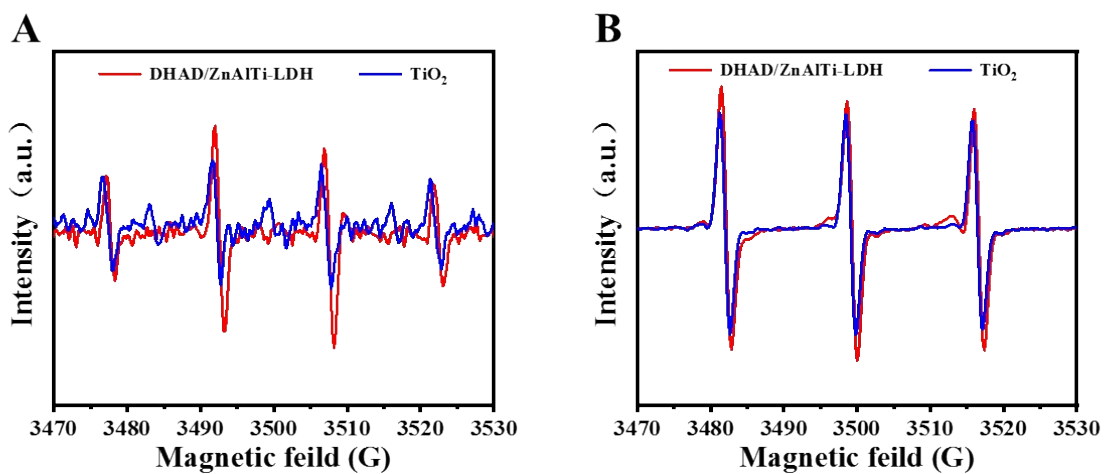


Figure S18. ESR spectra upon irradiation for detection of (A) $\cdot\text{OH}$, (B) $^1\text{O}_2$.

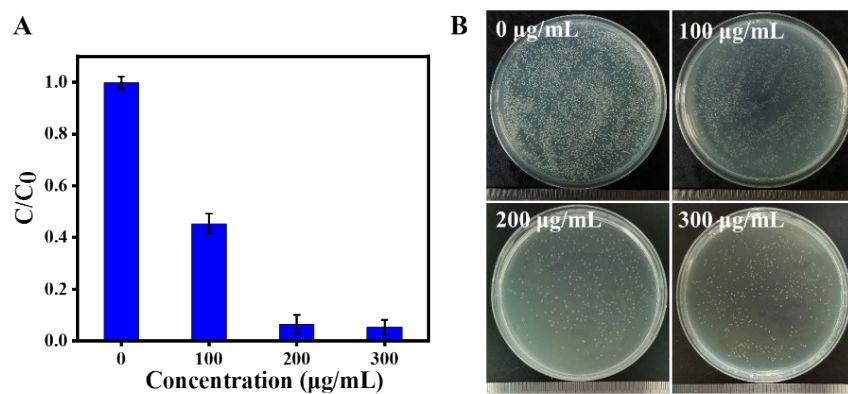


Figure S19. The antibacterial performance of different concentrations of DHAD/LDH against *S. aureus* under simulated light (A) and corresponding photographs (B). The inhibition rate of *S. aureus* was 54.6%, 91.8%, 93.2% treated with 100 µg mL⁻¹, 200 µg mL⁻¹ and 300 µg mL⁻¹ of DHAD/LDH, respectively.

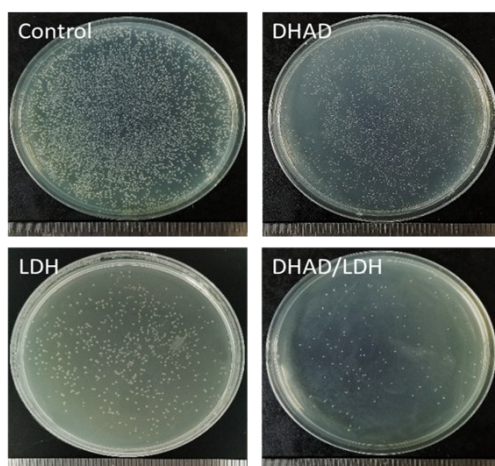


Figure S20. Photographs of antibacterial results for control and other groups after 40 min irradiation.

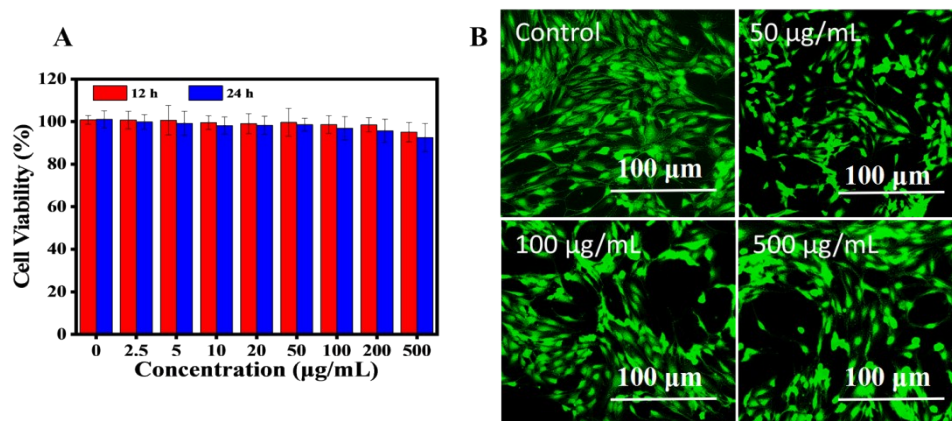


Figure S21. Cytotoxicity of DHAD/LDH in mouse renal epithelial cells (A) and the corresponding calcein-AM/PI staining images after 24 h incubation (B).

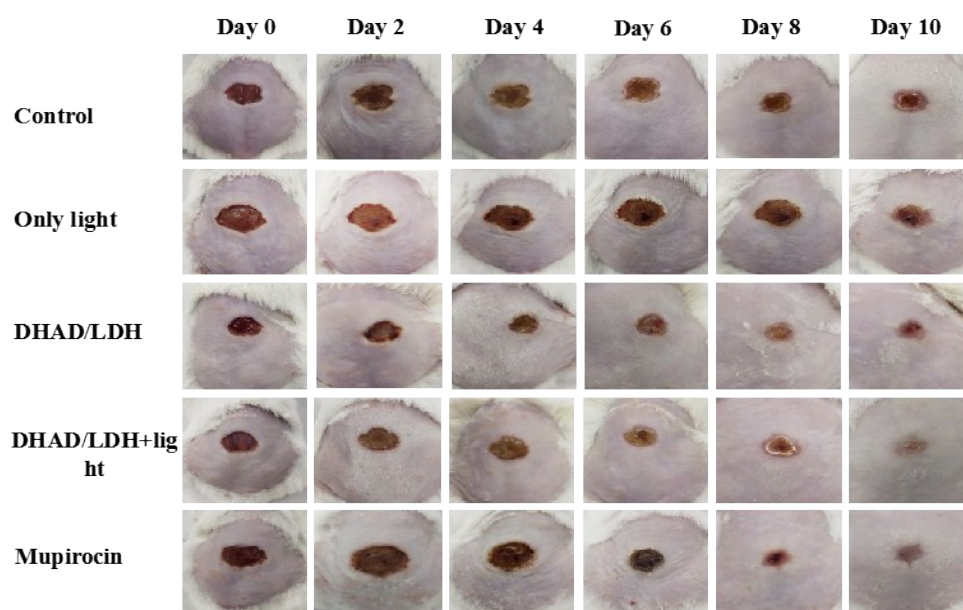


Figure S22. Photographs of the treatment process of different drugs on infected wounds.

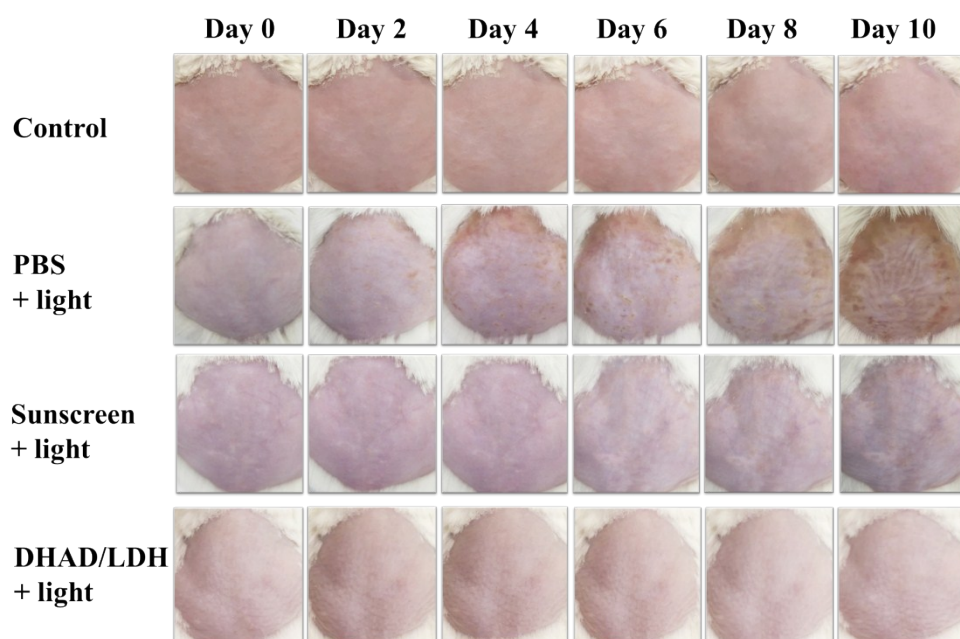


Figure S23. Photographs of UV-block performance treated with different groups for 10 days.

References

1. Y. Cui, E. Yasutomi, Y. Otani, K. Ido, T. Yoshinaga, K. Sawada and T. Ohwada, *Bioorg. Med. Chem.*, 2010, **18**, 8642–8659.
2. F. Li, L. Huang, Q. Li, X. Wang, X. Ma, C. Jiang, X. Zhou, W. Duan and F. Lei, *Molecules*, 2019, **24**, 4191.
3. L. Wang, X. Zhang, X. Yu, F. Gao, Z. Shen, X. Zhang, S. Ge, J. Liu, Z. Gu and C. Chen, *Adv. Mater.*, 2019, **31**, 1901965.